Machine-specific MRI quality control procedures for stereotactic radiosurgery treatment planning

Ali Fatemi, Ph.D.[1,2]; Somayeh Taghizadeh, M.S.[1,2]; Claus Chunli Yang, Ph.D.[1]; Madhava R. Kanakamedala, M.D.[1]; Srinivasan Vijayakumar, M.D.[1]; Roberto Rey-Dios, M.D.[1,3]; Bart Morris, M.S.[1]; William N. Duggar, M.S.[1]; Edward Florez, Ph.D.[2]

[1] Department of Radiation Oncology, University of Mississippi Medical Center, Jackson, MS, USA
[2] Department of Radiology, University of Mississippi Medical Center, Jackson, MS, USA
[3] Department of Neurosurgery, University of Mississippi Medical Center, Jackson, MS, USA

Abstract

Purpose
MR images are necessary for accurate contouring of intracranial targets, determination of gross target volume (GTV) and evaluation of organs at risk (OAR) during stereotactic radiosurgery (SRS) treatment planning procedures. Many centers use MRI simulators or regular diagnostic MRI machines for SRS treatment planning; while both types of machine require two stages of quality control (QC), both machine- and patient-specific, before use for SRS, no accepted guidelines for such QC currently exist. This article describes appropriate machine-specific QC procedures for SRS applications.

Methods and materials
We describe adaptation of American College of Radiology (ACR)-recommended QC tests using an ACR MRI phantom for SRS treatment planning. In addition, commercial Quasar MRID^{3D} and Quasar GRID^{3D} phantoms (Modus Medical, London, ON, Canada) were used to evaluate the effects of B_0 inhomogeneity, gradient nonlinearity, and a Leksell G frame (SRS frame) and its accessories on geometrical distortion in MR images.

Results
QC procedures found maximal in-plane distortions of 3.5 mm and 2.5 mm in the x and y directions, respectively, and < 1 mm distortion at a head-sized region of interest. MR images acquired using a Leksell G frame and localization devices showed a mean absolute deviation of 2.3 mm from isocenter. The results of modified ACR tests were all within recommended limits and baseline measurements have been defined for regular weekly QC tests.

Conclusions
With appropriate QC procedures in place, it is possible to obtain clinically useful MR image SRS treatment plans on a regular basis. MRI examination for SRS planning can benefit from the improved localization and planning possible with the superior image quality and soft tissue contrast achieved under optimal conditions.

Sequence/contrast	Parameters	Disease
Axial T1-weighted MPRAGE	1 x 1 x 1 mm^3, TR/TE = 2200/2.91 ms, 300 Hz/pixel	Brain metastasis, pituitary/parasellar lesions, acoustic neuroma/schwannoma, trigeminal neuralgia, AVM
Axial T2-weighted SPACE	0.9 x 0.9 x 1 mm^3, TR/TE = 1400/184 ms, 345 Hz/pixel	Pituitary/parasellar lesions, acoustic neuroma/schwannoma, AVM
Axial T2-weighted CISS	0.9 x 0.9 x 1 mm^3, TR/TE = 5.48/2.38 ms, 340 Hz/pixel	Pituitary/parasellar lesions, acoustic neuroma/schwannoma, trigeminal neuralgia

Table 1:
Approved MRI pulse sequences for SRS treatment planning.

Abbreviations: MPRAGE = magnetization-prepared 180-degree radio-frequency pulses and rapid gradient-echo; SPACE = sampling perfection with application optimized contrasts using different flip angle evolution; CISS = Three-dimensional (3D) constructive interference in steady state; TR = Time of Repetition; TE = Time of Echo

Introduction

Using MR images for stereotactic radiosurgery (SRS) treatment planning requires careful consideration of a number of factors [1], including choice of the correct MRI pulse sequences (3D, no slice gap, less geometrical distortion, high signal-to-noise ratio (SNR) and isotropic spatial resolution), immobilization devices (MRI-compatible SRS frame), customized RF coils (proper sensitivity, low RF deposition, consequently less contour deformation) such as a single channel send-and-receive RF head coil (Rx/Tx RF head coil), and most importantly, confirmation that the MRI images acquired possess high geometrical accuracy and stability.

Existing MR quality control (QC) procedures [2–6] are inadequate for assessing MRI scanners for SRS treatment-planning purposes, primarily because existing tests have been developed for machines used in general diagnostic radiology. There, the goal is to maintain image quality rather than spatial fidelity and signal intensity [7]. Several well-established references from the American College of Radiology (ACR) [2, 3] and the American Association of Physicists in Medicine (AAPM) [4–6] provide guidance regarding QC procedures for MRI scanners used in diagnostic radiology, but no guidance documents currently describe the unique QC factors that must be considered when using MRI scanners in SRS treatment planning [7–9]. However, existing quality

Daily QA (MRI technologists) using ACR phantom	**Monthly QA (Therapy physicist/MRI physicist) using MRID^{3D}, GRID^{3D}, and ACR phantoms**	**Annual QA (MRI physicist) using MRID^{3D}, GRID^{3D}, and ACR phantoms**
Inspect bore for loose metal (bobby pins, earrings, etc.)	Patient safety (monitors, intercom, panic ball, emergency buttons, and signage)	20-channel RF coil integrity check
Tx/Rx and 20-channel RF coil SRS check using uniform phantom	Patient comfort (bore light and fan)	B_0 constancy
Patient safety (intercom, panic ball, detector)	Percent signal ghosting	B_{1+} constancy
Geometry accuracy and B_0 check using ACR phantom	Percent image uniformity	Gradient linearity constancy
	High/low contrast accuracy	Slice thickness accuracy
Weekly QA (MRI technologists) using ACR phantom	Coach position accuracy	Slice position accuracy
Transmitter gain constancy	Image artifact	Geometrical accuracy
Center frequency constancy	Geometrical accuracy (large field-of-view)	Rx/Tx RF head coil check
20-channel RF head coil SNR	Geometrical accuracy (small field-of-view) with and without frame	20-channel RF head coil check
Rx/Tx RF head coil SNR		Dynamic field map
Slice thickness accuracy		Eddy current compensation
Slice position accuracy		Gradient delay
Geometric accuracy and B_0 check using ACR phantom		Gradient sensitivity
		Body coil image brightness
		Magnet shim
		Rx gain calibration
		Body coil tuning
		Spike
		PMU transmit
		Rx stability
		Tx stability

Table 2 :
QC tests and frequencies for MRI guided Stereotactic Radiosurgery (SRS).

Abbreviations: Tx/Rx RF coil = single channel send/receive radio-frequency coil; PMU = Phasor Measurement Unit

Test	MRI machine tolerance
MRI geometrical distortion	
Evaluate distortion vector, combined effect (B_0 inhomogeneity and gradient nonlinearity) over large field-of-view (37 cm)	< 1 mm over 20 cm DSV and < 2 mm over 37 cm DSV
Evaluate B_0 inhomogeneity over large field-of-view (37 cm)	2 ppm
Evaluate the geometrical distortion vector with stereotactic frame (small field-of-view, 20 cm)	< 1 mm
Adapted ACR QC tests	
Setup and table position accuracy	< 1 mm
Center frequency	Pass/Fail
Signal ghosting	≤ 2.5%
Transmitter gain or attenuation	Pass/Fail
High contrast spatial resolution	Row and column resolution ≤ 1 mm
Low contrast detectability	9 rows total for up to 1.5T
Magnetic field homogeneity	Action limit ± 2 ppm
Artifact evaluation	Pass/Fail
Magnetic field homogeneity	Action limit ± 2 ppm
Geometrical accuracy	Within < 1.5 mm of actual length
Visual checklist	Pass/Fail
Slice position accuracy	Difference from actual position ≤ 3 mm
Slice thickness accuracy	Action limit is 5 ± 0.7 mm
20-channel RF head coil evaluation	Signal-to-noise ratio (SNR) PIU ≥ 87.5% (< 3T) Percentage Signal Ghosting (PSG) ≤ 2.5%
Rx/Tx RF head coil evaluation	Signal-to-noise ratio (SNR) PIU ≥ 87.5% (< 3T) Percentage Signal Ghosting (PSG) ≤ 2.5%
Rx/Tx RF head coil check	Pass/Fail
20-channel RF head coil check	Pass/Fail
Dynamic field map	Pass/Fail
Eddy current compensation	Pass/Fail
Gradient delay	Pass/Fail
Gradient sensitivity	Pass/Fail
Body coil image brightness	Pass/Fail
Magnet shim	Pass/Fail
RX gain calibration	Pass/Fail
Body coil tuning	Pass/Fail
Spike	Pass/Fail
PMU transmit	Pass/Fail
Rx stability	Pass/Fail
Tx stability	Pass/Fail
Assessment of MRI safety program	**Pass/Fail**

Table 3 :
Summary of MRI acceptance QC tests for SRS treatment planning.

Abbreviations: DSV = Diameter Spherical Volume; PIU = Percentage Image Uniformity control tests can be modified to provide the necessary information for a given SRS-planning application by testing over appropriate volumes and using SRS-specific MR imaging parameters.

Development of our QC process started with evaluation of gross machine factors, including B_0 inhomogeneity and gradient non-linearity, over a large field-of-view using the scanner body coil, then narrowed to study the effects on geometrical stability of MR images due to use of an MRI-compatible SRS frame and its localizer using a Tx/Rx RF head coil [10]. Finally, adapted ACR tests were performed to evaluate the image contrast, spatial resolution, gradient stability for accurate slice selection and thickness, RF coil sensitivity, and acquisition of artifact-free MR images. Testing these factors ensures that acquired images possess the quality and resolution required for precision SRS treatment planning, accurately identifying disease extent and proximity relative to adjacent organs at risk (OAR) [1].

We are establishing a quality assurance (QA) program to continuously and systematically evaluate MRI scanner performance, safety and stability for SRS treatment planning. Our goal in this article is to describe our QC tests and strategy in establishing a QA program for MRI-guided SRS treatment planning. This paper focuses narrowly on MRI machine-specific aspects of the QC procedure and leaves patient-specific QC tests, including patient-specific geometrical distortion evaluation, correction methods, customized RF coils, patient comfort, MRI safety, and MRI pulse sequence optimization, for future reports.

Method and materials

We recently installed a Leksell Gamma Knife® Icon™ SRS treatment unit[1] (Elekta AB, Stockholm, Sweden) and a 1.5T MAGNETOM Aera RT Pro edition (Siemens Healthcare, Erlangen, Germany) MRI machine at our institute. The SRS committee consists of three physicists, a radiologist, a radiation oncologist, and a neurosurgeon, who work together to develop guidelines for MRI-guided SRS treatment planning. MR images are used to assess cases of brain metastasis, pituitary/parasellar lesions, acoustic neuroma, trigeminal neuralgia, and arteriovenous malformation (AVM).

The MRI SRS QC procedure has been developed based on factors including imaging site, MRI pulse sequence(s), adapted or standard RF coils, and any immobilization devices required. SRS patients are scanned on a regular diagnostic MRI table, using a Leksell G frame with immobilization and localization devices, or frameless, as appropriate. In our institute, we use a Tx/Rx CP head coil (Siemens Healthcare, Erlangen, Germany) to fit the Leksell G frame, plus an MRI indicator box with an adaptor to the coil, and are still able to keep the specific absorption rate (SAR) under 3 W/kg. The downside of using such an RF coil is a less-than-ideal SNR and long scanning time; thus, we use a regular 20-channel RF head coil for frameless cases. MRI pulse sequences have been evaluated by the SRS committee based on disease site and treatment planning criteria detailed in Table 1.

We summarize the commissioning and quality control (QC) tests (test, frequency, and machine tolerance) in Tables 2 and 3.

1. Evaluation of geometrical distortion over a large field-of-view

We used a QUASAR™ MRID^{3D} (Modus Medical, London, ON, Canada) geometrical distortion phantom (Fig. 1) to measure B_0 inhomogeneity and gradient non-linearity using a reverse gradient technique over a 37 x 32 cm (W x L) phantom area. The phantom was scanned with a 3D VIBE T1-weighted sequence: 1 mm^3 isotropic voxels, NEX of 2, TE of 4 ms, TR of 9 ms, a flip angle ~10°, and a bandwidth of 120 Hz/pixel. QUASAR™ MRID^{3D} comes with easy-to-use image analysis software for calculation of the phantom boundary distortion vector field, volumetric 3D distortion vector field, and B_0 distortion vs. gradient distortion, using 3D spherical harmonic analysis.

[1] The information shown herein refers to products of 3rd party manufacturer's and thus are in their regulatory responsibility. Please contact the 3rd party manufacturer for further information.

Figure 1:
Quasar MRID^{3D} geometrical distortion phantom

Figure 2:
(2A) Quasar GRID^{3D} image distortion phantom
(2B) Standard ACR

2. Evaluation of the effect of an SRS frame and localizer on geometrical stability of MR images

We used a QUASAR™ GRID^{3D} Image Distortion Phantom and analysis system (Modus Medical, London, ON, Canada) to evaluate MR image distortion due to the introduction of an SRS frame and localizers. The system is comprised of a phantom and analysis software which work together to produce a 3D map of spatial distortion with submillimeter accuracy throughout a volume of interest. The phantom (Fig. 2A) is an acrylic cube containing a 1-cm 3D grid of channels filled with copper sulfate solution. The region of interest is a 14 x 13 x 11 cm^3 volume containing 2002 vertex locations, the positions of which are known to within 0.1 mm.

The phantom accurately and reproducibly mounts securely to the SRS Leksell Frame G at a known position. It fits within both the Leksell® MR Indicator and Leksell® CT Indicator. We scanned our phantom using a 3D MPRAGE pulse sequence: T1-weighted, 1 x 1 x 1 mm^3, TR/TE of 2200/3.74 ms, and 350 Hz/pixel. The MPRAGE is the only MRI pulse sequence being used for treatment planning and the rest of the sequences will be registered rigidly.

3. ACR MRI tests adapted for SRS treatment planning

We used a standard MRI ACR phantom (Fig. 2B) to evaluate the rest of our adapted QC MRI tests. The ACR phantom has been scanned based on MRI pulse sequences and parameters summarized in Table 4. All QC tests with their tolerances are summarized in Table 2.

Protocol	Phantom used	TR (ms)	TE (ms)	FOV (mm)	# Slices	Slice thickness (mm)	GAP	NEX	Matrix	BW
ACR T1 Localizer	ACR	200	20	25	1	20	N/A	1	256 x 256	Routine (15.6 kHz)
ACR T1 Axial	ACR	500	20	25	11	5	5	1	256 x 256	Routine (15.6 kHz)
ACR T2 Axial	ACR	2000	20/80	25	11	5	5	1	256 x 256	Routine (15.6 kHz)
Site T1 Axial	ACR	Site protocol	Site protocol	25	11	5	5	Site protocol	256 x 256	Site protocol BW
Site T2 Axial	ACR	Site protocol	Site protocol	25	11	5	5	Site protocol	256 x 256	Site protocol BW
Low BW Axial[1]	ACR	500	20	25	1	5	N/A	1	256 x 256	Minimum BW @ 256 x 256 matrix
Low BW Coronal[1]	ACR	500	20	25	1	5	N/A	1	256 x 256	Minimum BW @ 256 x 256 matrix
Low BW Sagittal[1]	ACR	500	20	25	1	5	N/A	1	256 x 256	Minimum BW @ 256 x 256 matrix
High BW Axial[1]	ACR	500	20	25	1	5	N/A	1	256 x 256	Minimum BW @ 256 x 256 matrix
High BW Coronal[1]	ACR	500	20	25	1	5	N/A	1	256 x 256	Minimum BW @ 256 x 256 matrix
High BW Sagittal[1]	ACR	500	20	25	1	5	N/A	1	256 x 256	Minimum BW @ 256 x 256 matrix

Table 4 :
MRI pulse sequences and parameters for adapted MRI ACR QC tests.

Abbreviations: BW = Bandwidth

[1] Acquired three separate series, each consisting of a single image through the center of phantom with minimum and highest bandwidths.

4. Evaluating MRI safety

As part of our acceptance tests we used a gauss meter to carefully map and post the 5-gauss line with proper signage. We monitor all patients through both a questionnaire and in-person consultation to make sure that any person with a cardiac pacemaker or neurosimulators does not cross the 5-gauss line. Our MRI room is also equipped with a Ferroguard® (Metrasens Ltd., Lemont, IL, USA) wall mounted system deployed in an entryway mode on both sides of the doorway. This system provides real-time monitoring of the local ferromagnetic environment with an audible alert system. We also check the patient/console intercom system, table-top button (magnet housing and console), emergency stop buttons, emergency rundown unit, and door switches on a regular basis.

5. Establishing MRI quality assurance program

We summarize our proposed QC tests and their frequencies in Table 2. What follows is a formulaic approach to monitor B_0 inhomogeneity and geometrical distortion with weekly and daily QC tests using an ACR phantom. We found that incorporating these tests into recommended weekly ACR tests run by a technologist and using only an MRI ACR phantom makes the process faster and more efficient in our busy clinic.

First, we defined our reference B_0 inhomogeneity and geometrical distortion during monthly and commissioning processes using Quasar MRID^{3D}. The MRI image geometrical distortion and machine B_0 inhomogeneity were defined over a 37 x 32 cm (W x L) area on three dimensions (Δx, Δy, Δz) and absolute value from MRI isocenter. Next, we scanned the regular ACR MRI phantom and defined B_0 inhomogeneity using a bandwidth difference technique, and defined geometrical distortion using sagittal slices 1 and 5 for all three dimensions. We used geometrical distortion measurements for slice 5 (Δx, Δy) and the sagittal plane (Δz) for baseline calculation, assuming that slice 5 is at or very close to the MRI isocenter. Finally, the average baseline was defined based on equation 1 and 2 for the same slices and diameter on both MRID^{3D} and ACR phantoms. The baseline measure is used for weekly checks, and we define our tolerance as 2% changes, and action level as a measured 4% difference.

Equation 1:

$$\text{Base}_{B0} = \text{ACR}_{B0} - \text{MRID}^{3D}_{B0}$$

Base$_{B0}$ is an averaged B_0 inhomogeneity at the same slice at MRID^{3D} and ACR phantoms; *MRID$^{3D}_{B0}$* is the measured average B_0 inhomogeneity in ppm; and *ACR$_{B0}$* is averaged B_0 inhomogeneity in (ppm) using the bandwidth difference technique, and

Equation 2:

$$\text{Base}_{\text{geometrical distortion}} = \text{ACR}_{\text{geometrical distortion}} - \text{MRID}^{3D}_{\text{geometrical distortion}}$$

Where Base$_{\text{geometrical distortion}}$ is the geometrical distortion at the slice and orientation at MRID^{3D} and ACR phantoms; ACR$_{\text{geometrical distortion}}$ is the measured geometrical distortion at slice 5 and sagittal plane on all three directions (Δx, Δy, Δz); and MRID$^{3D}_{\text{geometrical distortion}}$ is the measured geometrical distortion at the same ACR slice and orientation.

Results

The geometrical distortion over a 37 x 32 cm (W x L) area was evaluated in all three dimensions (Δx, Δy, Δz), absolute distance from MRI isocenter. Table 5 contains summary statistics; the maximum distortion in the x and y plane (axial plane) was 3.5 mm and 2.5 mm at the boundaries.

The detailed measurements along all three coordinates and their absolute values with respect to MRI isocenter is shown in Figure 3. The B_0 inhomogeneity along the z direction was measured separately using an inverse gradient technique, and those data are also shown in Figure 3.

We used a QUASAR™ GRID^{3D} Image Distortion Phantom and analysis system to evaluate image distortion in MR images due to the presence of an SRS frame and localizers. The data in the axial plane of the MR images showed a maximum of 0.5 mm in the x-direction, 1.5 mm in the y-direction; in the z-direction the maximum of 2.6 mm was observed at the phantom boundary (11 cm from MRI isocenter). The results showed a mean absolute deviation of 2.3 mm from isocenter. We defined our ACR phantom weekly B_0 inhomogeneity and geometrical distortion baselines: the reference B_0 inhomogeneity using MRID^{3D} phantom was evaluated on all three axes (axial: 1.89 ppm, coronal: 0.135 ppm and sagittal: 0.068 ppm) as well as on average (0.699 ppm), all well-defined within our limits of ± 2 ppm. The Base$_{B0\ \text{inhomogeneity}}$ based on Equation 1 was defined as 0.03 ppm.
The Base$_{\text{geometrical distortion}}$ was defined for our MRI ACR phantom at slice 5 as 0.6 mm in the x-direction, 0.8 mm in the y-direction, and 0.5 mm in the sagittal plane.

Continued on page 92.

	Mean (mm)	STD (mm)	Max (mm)	> 2.5 mm (%)
dx	0.91	0.67	3.5	3
dy	0.52	0.39	2.51	0
dz	2.38	2.45	13.1	34
dr	2.79	2.36	13.19	40

Table 5 :
Summary statistical of MRID3D geometrical distortion measurements.

Abbreviations: STD = Standard Deviation

3

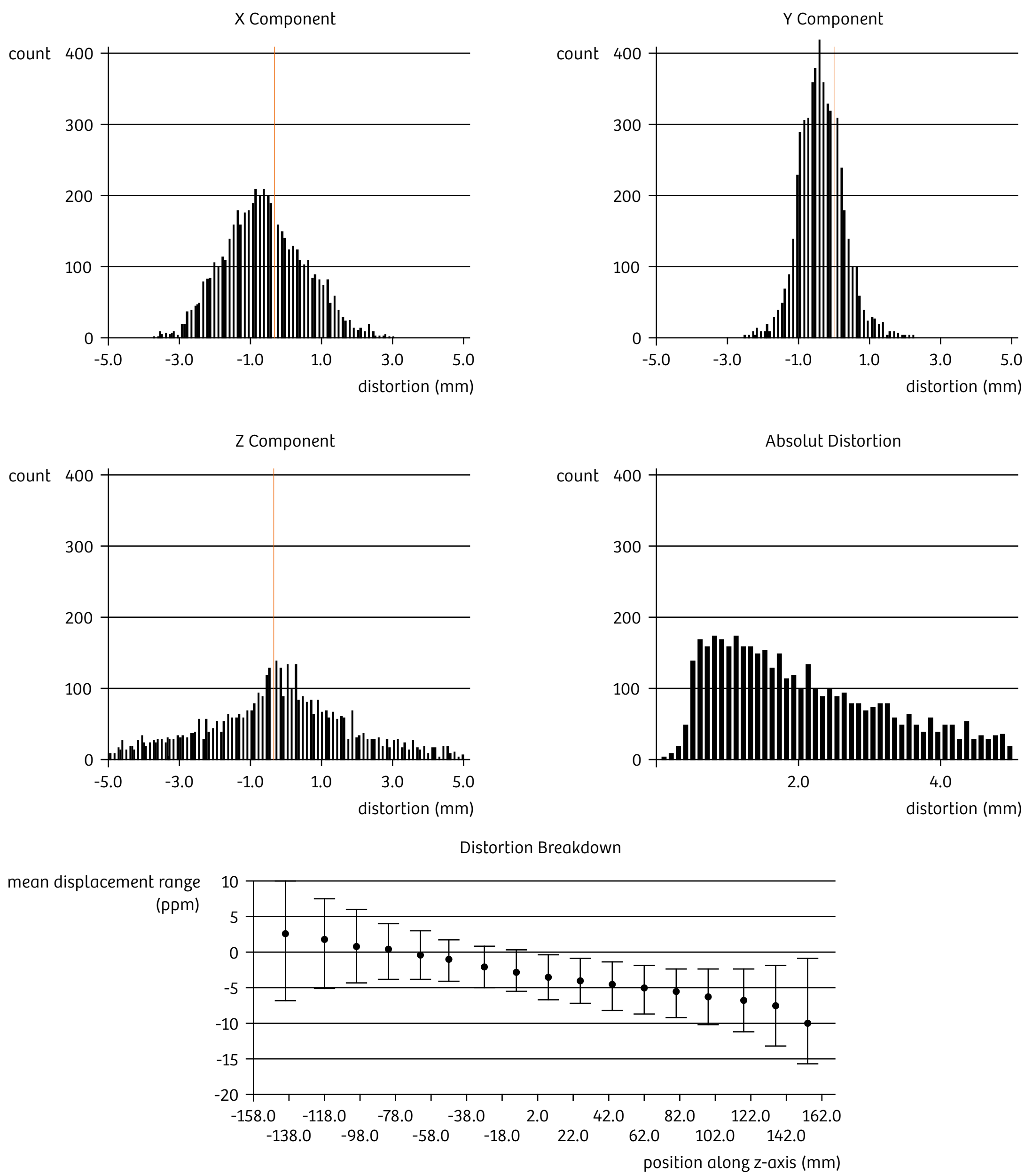

Figure 3:
B_0 inhomogeneity and distortion measurement results using an MRID3D phantom.

MRI equipment evaluation summary		
1.	Setup and table position accuracy	Pass
2.	Center frequency	Pass
3.	Transmitter gain or attenuation	Pass
4.	Geometric accuracy measurements	Pass
5.	High-contrast spatial resolution	Pass
6.	Low-contrast detectability	Pass
7.	Artifact evaluation	Pass
8.	Visual checklist	Pass
9.	Magnetic field homogeneity	Pass
	Method of testing	BW diff
10.	Slice-position accuracy	Pass
11.	Slice-thickness accuracy	Pass
12.	Radiofrequency coil checks (20-channel RF head coil)	
	a. SNR	Pass
	b. Volume coil percent image uniformity	Pass
	c. Percent signal ghosting	Pass
13.	Radiofrequency coil checks (Rx/Tx RF head coil)	
	a. SNR	Pass
	b. Volume coil percent image uniformity (PIU)	Pass
	c. Percent signal ghosting	Pass
14.	Rx/Tx RF head coil check	Pass
15.	20-channel RF head coil check	Pass
16.	Dynamic field map	Pass
17.	Eddy current compensation	Pass
18.	Gradient delay	Pass
19.	Gradient sensitivity	Pass
20.	Body coil image brightness	Pass
21.	Magnet shim	Pass
22.	RX gain calibration	Pass
23.	Body coil tuning	Pass
24.	Spike	Pass
25.	PMU transmit	Pass
26.	Rx stability	Pass
27.	Tx stability	Pass

Table 6 :
MRI SRS QC results.

Abbreviations: PMU = Phasor Measurement Unit

All adopted ACR measures were within our defined tolerance, as summarized in Table 6. Specifically, the 20-channel and Rx/Tx RF head coils have been tested thoroughly for SNR, PIU and PSG, and the results were found to fall within our accepted limits.

Discussion

The methodology discussed herein describes practical strategies we have implemented through lessons learned performing clinical MRI QA and SRS treatment planning [11–14]. We focus on discussion of major issues encountered during our QC procedures.

The MRI machine specifications which have the greatest potential to affect SRS treatment planning are B_0 and B_1 inhomogeneity and gradient non-linearity, which affect the geometrical accuracy and intensity uniformity of MR images. Use of single channel Rx/Tx RF head coils, a Leksell G frame (SRS frame) and accessories for SRS treatment planning only exacerbates these issues. Using an MRID^{3D} phantom over a 37 x 32 cm (W x L) area gives enough information about MR image distortion due to B_0 inhomogeneity and gradient non-linearity to allow acquired images to be used for SRS treatment planning. As we expected, geometrical distortion is within 1 mm accuracy in the axial plane (x and y directions), and 2 mm along the z direction 10 cm from isocenter (almost head size), but it worsens to the order of 5 mm at the boundaries (16 cm away from isocenter).

Immobilization devices constructed from materials optimized for radiation therapy may not necessarily be optimal for MRI (e.g. carbon fiber) [15–17]. In our experience, it is no longer sufficient for immobilization device materials (Leksell G frame, screws, adaptor, and MRI localizer) to be simply MRI-compatible; these materials and devices should be MRI-optimal. Poor material choices can contribute to magnetic susceptibility induced geometric distortions. Our phantom results specifically on 3D axial T2 SPACE and axial T2 CISS sequences show artifacts even after pulse sequence optimization and use of different orientations. It is essential that some MRI sequences reviewed by the SRS team be repeated using a different sequence, such as 2D axial T2 or T1-weighted Turbo Spin Echo (TSE). However, our results from Quasar™ GRID^{3D} shows that images acceptable for treatment planning can be obtained with the use of Laksell frame and localization devices by using the right MRI pulse sequence and a Tx/Rx RF head coil.

Our proposed SRS MRI QA program has been reviewed and approved by our QA committee, and peer reviewed at every step by SRS committee members. Our aim is to minimize the scanning time and maximize efficiency.

One major change proposed was use of the MRI ACR phantom for weekly geometrical accuracy checks rather than the MRID^{3D}. This streamlines the process and the technologist can incorporate these results into the regular weekly checks.

Our results indicated that gradient nonlinearity-induced geometric distortions can be severe and must be corrected using 3D distortion correction prior to using MR images for SRS treatment planning. However, even with 3D distortion correction, residual distortions can persist for large FOV prescriptions. One compounding factor is that some MRI scanners permit acquisition of image volumes positioned off-center from isocenter in the superior/inferior direction. This approach increases the likelihood of scanning in regions of nonlinear gradients and, therefore, increases the likelihood of residual distortions. At a minimum, the magnitude of these residual distortions should be characterized as a function of radial distance from isocenter for each scanner. Ideally, the residual distortions would be corrected.

High MR image intensity uniformity is critical in SRS treatment planning. Phased-array RF coils require correction for differences in the sensitivity profiles of each coil element during reconstruction to optimize image uniformity. These corrections, often based on a quick prescan image, become increasingly important when flexible phased-array RF coils, wrapped around the patient in various positions, are utilized. Our results indicate that by using prescan normalization and postprocessing corrections the MR images collected are within preset limits and SNR, PIU and PSG tests serve as good indications for variation.

The participation of the dedicated SRS team, including the medical physicist, radiation oncologist, and neurosurgeon in the quantification, protocol modification and development of quality assurance procedures, as well as verification of MRI data used for SRS planning, is critical. Moreover, the scanner selection considerations, specifications, chosen MRI pulse sequences, and post processing packages are extremely important in having a successful program of MRI-guided SRS treatment planning.

Conclusions

In conclusion, we describe an MRI machine QC procedure to maintain clinically acceptable MR image acquisition for SRS treatment planning purposes. MRI examinations for SRS planning can benefit from the improved localization and planning possible with the superior image quality and soft tissue contrast achieved with appropriate MRI QA. We recommend convening a team of experts who meet periodically to review cases, discuss new MRI pulse sequences and technology, including newly available post-processing software packages, and who can develop a custom QA program for the facility. We strongly believe this type of dialog opens opportunities for greater use of MRI images in SRS treatment planning, especially in a new era of MRI-guided radiotherapy available in commercial machines.

Acknowledgments

The authors would like to thank Brain Barker and especially all members of the MRI service crew for fruitful discussions.

References

1 P. M. Evans, Anatomical imaging for radiotherapy, Phys. Med. Biol. 2008, 53, R151–R191.
2 American College of Radiology (ACR). Magnetic resonance imaging quality control manual. 2015.
3 American College of Radiology (ACR). MR accreditation program phantom test guidance. 2005.
4 American Association of Physicists in Medicine (AAPM). AAPM Report 28: Quality assurance methods and phantoms for magnetic resonance imaging. 1990.
5 American Association of Physicists in Medicine (AAPM). AAPM Report 34: Acceptance testing of magnetic resonance imaging systems. 1992.
6 American Association of Physicists in Medicine (AAPM). AAPM Report 100: Acceptance testing and quality assurance procedures for magnetic resonance imaging facilities. 2010.
7 V. S. Khoo and D. L. Joon, New developments in MRI for target volume delineation in radiotherapy, Br. J. Radiol. 2006,79, S2–S15.
8 P. Metcalfe, G. P. Liney, L. Holloway, A. Walker, M. Barton, G. P. Delaney, S. Vinod, and W. Tome, The potential for an enhanced role for MRI in radiation-therapy treatment planning, Techol. Cancer Res. Treat. 2013, 12, 429–446.
9 S. Hanvey, A. H. Sadozye, M. McJury, M. Glegg, and J. Foster, The influence of MRI scan position on image registration accuracy, target delineation, and calculated dose in prostatic radiotherapy, Br. J. Radiol. 2012, 1256–1262.
10 B. Belaroussi, J. Milles, S. Carme, Y. M. Zhu, and H. Benoit-Cattin, Intensity non-uniformity correction in MRI: Existing methods and their validation, Med. Image Anal. 2006, 10, 234–246.
11 Y. Wang, P. J. Rossman, R. C. Grimm, S. J. Riederer, and R. L. Ehman, Navigator-echo-based real-time respiratory gating and triggering for reduction of respiration effects in three-dimensional coronary MR angiography, Radiology, 1996, 198, 55–60.
12 A. Fransson, P. Andreo, and R. Potter, Aspects of MR image distortions in radiotherapy treatment planning, Strahlenther. Onkol. 2001, 177, 59–73.
13 American Association of Physicists in Medicine (AAPM). Comprehensive QA for radiation oncology: Report of AAPM Radiation Therapy Committee Task Group 40, Med. Phys. 1994, 31, 581–618
14 P. Jezzard and S. Claire, “Sources of distortion in functional MRI data,” Hum. Brain Mapp.1999, 8, 80–85.
15 N. Baldwin, K. Wachowicz, and B. G. Fallone, A two-step scheme for distortion rectification of magnetic resonance images, Med. Phys.2009, 36, 3917–3926.
16 M. L. Kessler, Image registration and data fusion in radiation therapy, Brit. J. Radiol. 2006, 79, S99–S108.
17 S. Devic, MRI simulation for radiotherapy treatment planning, Med. Phys. 2012, 39(11), 6701–6711.

The concepts and information presented in this paper are based on research and are not commercially available.

Contact

Ali Fatemi, Ph.D., MCCPM
Senior physicist, Director of MR Guided Radiotherapy Lab, Assistant professor
Departments of Radiology and Radiation Oncology
University of Mississippi Medical Center

2500 North State Street
Jackson, Mississippi 39216
USA
Phone: +1 (601)345-0135
afatemi@umc.edu

Learn more!

From technology to clinical applications and protocols, you will find all the latest news about Siemens Healthineers MR in Radiation Oncology at

www.siemens.com/magnetom-world-rt

MRI in Radiation Therapy
Peer-to-peer exchange of protocols, articles and tips

Overview Protocols Application Tips Articles & Case Studies Talks & Keynotes

The MAGNETOM World is the community of Siemens MR users worldwide, providing you with relevant clinical information. Here you will find application tips and protocols to optimize your daily work. Lectures and presentations from experts in the field will allow you to be exposed to new ideas and alternative clinical approaches.

Put the advantages of the MAGNETOM World to work for you!